RECENT CLIMATE CHANGE IMPACT ON EAST ASIA RENEWABLE ENERGY RESOURCES

An Undergraduate Research Scholars Thesis

by

ZONGHUI LI

Submitted to the Undergraduate Research Scholars program at
Texas A&M University
in partial fulfillment of the requirements for the designation as an

UNDERGRADUATE RESEARCH SCHOLAR

Approved by Research Advisors: Dr. Yangyang Xu
Dr. Don T. Conlee

May 2019

Major: Environmental Studies

TABLE OF CONTENTS

ABSTRACT

Recent Century Climate Change's Impact on East Asia Renewable Energy Resources

Zonghui Li
Environmental Programs
Texas A&M University

Dr. Yangyang Xu
Department of Atmospheric Sciences
Texas A&M University

Dr. Don T. Conlee
Department of Atmospheric Sciences
Texas A&M University

This research aims to identify the climate change and air pollution emissions impact on renewable energy resources, specifically for solar energy availability. We analyzed meteorological reanalysis data of solar radiation over the last 30-50 years, on the areas that are directly impacted by Eastern Asian Summer Monsoon (EASM) such as southeastern China, and other parts of China and countries in East Asia. We identify changes in solar energy availability, which includes lower solar radiation arriving at the surface that will likely produce less solar energy. This research also compiles the locations of current and planned solar energy programs and focuses analysis on the area with those programs. In the end, this research will discuss what anthropogenic influences of both climate and pollution mean for solar energy in China.

ACKNOWLEDGEMENTS

I would like to thank my research advisors and mentors, Dr. Xu and Dr. Conlee, for their support and guidance throughout the year of this research.

Thanks also go to my friends and classmates and the department faculty and staff for making my time at Texas A&M University a wonderful experience. Thanks to Chenrui Diao, for his support and guidance on the computing technique of this research.

Finally, thanks to my mother, Aizhen Wang, and father, Xin Li for their support and encouragement and to Zhuyu Yao for her love and patience.

NOMENCLATURE

EASM	East Asian Summer Monsoon
IEA	International Energy Agency
ITCZ	Inter-Tropical Convergence Zone
SCS	South China Sea
SST	Sea Surface Temperature

CHAPTER I

INTRODUCTION

The present paper is studying climate change impact on renewable energy, specifically solar power through 20th and 21st century. Because changes in the EASM affect cloud cover, it is essential to know if climate change has an impact on EASM and thus solar resources. Current research has mainly focused on analyzing changes in the EASM and provide strong evidence that climate change is making an impact on EASM. By comparing changes in solar radiation, and locations of renewable energy resources program, this research not only shows climate changes are making an impact on EASM, but also suggests the implications for renewable energy which is brought by this climate change. This research is building models and graphs of solar radiation arriving at the surface currently, which are helpful for renewable energy development in East Asia and most specifically China in the future.

EASM is caused by thermal contrast between Eurasia land and Pacific Ocean which both are the largest in the world (Wang et al. 2008), therefore EASM has two primary factors related to its physical process and mechanism: Pacific and Indian ocean SSTs and snow cover in the Eurasia and Tibetan Plateau (Ding and Chan 2005). EASM is part of the Asian Summer Monsoon, which includes both EASM and South Asian Monsoon. The South Asian Monsoon is more affected by thermal contrast between Indian Subcontinent and the Indian Ocean, the shift of the ITCZ, and the high-pressure system over the Indian Ocean and Tibetan Plateau over summer. Blocking highs over Eurasia land and subtropical high over Pacific over summer affects the hydrological circulation and this variability affects the activity of EASM (Ding and Chan 2005). EASM brings moisture to Yangtze River Basin in early May, and it affects precipitation,

cloud cover, and solar radiation in other areas later on through the year. The length of the rainy season, total rainfall and temperature reflect the change of EASM through 20th and 21st century, and changes in these factors affect incoming solar irradiance at the surface which eventually influences the collection of solar energy.

Anthropic activities influence global climate by human-caused deforestation, overuse of natural resources, increase greenhouse emission, etc., which are factors resulting in global warming. Figure 1 shows a dramatic increase in temperature anomaly globally between 1880 and 2018. Increase in temperature affects both thermal contrast and atmospheric circulation in East Asia by increasing the high-pressure system effect over Tibetan Plateau and the Pacific Ocean which results in precipitation changes in different regions. Table 1 shows data analysis completed by Burke and Scott (2017), dividing China in seven areas (Figure 2): North East (NE), Central West (CW),North Central China(NCC), North East Coast(NEC),South Central China(SCC), South East Coast(SEC) and South East(SE) (Burke and Scott 2017). Burke and

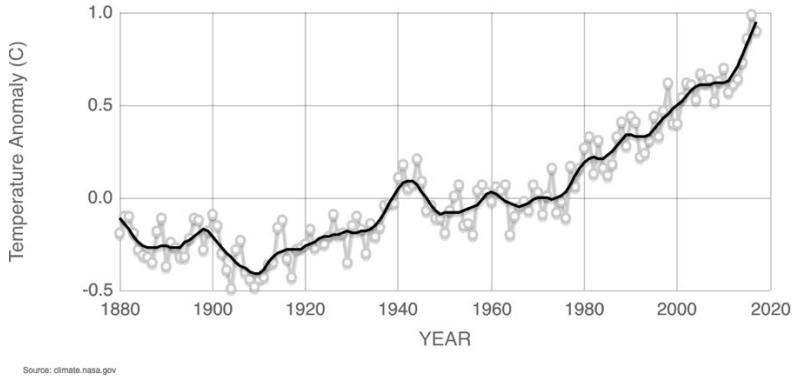

Figure 1 Global Temperature Anomaly (NASA 2017)

Table 1 Rainfall Data of seven areas in China (Burke and Scott 2017)

Variable		NE	NCC	NEC	CW	SCC	SEC	SE
Total rainfall	ΔP mean	0.8 ± 0.01	0.8 ± 0.01	0.9 ± 0.01	0.9 ± 0.03	0.6 ± 0.03	0.8 ± 0.01	0.6 ± 0.02
	Mean change (mm)	−28.3 ± 1.72	−34.9 ± 2.26	−13.5 ± 2.38	−13.3 ± 4.62	−110.0 ± 6.56	−72.9 ± 4.12	−146.2 ± 9.15
	ΔP 10th percentile	0.9 ± 0.01	0.9 ± 0.01	1.0 ± 0.01	1.0 ± 0.01	0.8 ± 0.01	0.9 ± 0.01	0.9 ± 0.01
	Mean change (mm)	−23.4 ± 1.82	−33.9 ± 2.93	−14.5 ± 2.49	−13.3 ± 4.98	−98.3 ± 6.44	−48.65 ± 3.27	−108.1 ± 7.87
Dry days	ΔP mean	1.2 ± 0.01	1.3 ± 0.02	1.2 ± 0.01	1.1 ± 0.04	1.5 ± 0.02	1.4 ± 0.01	1.6 ± 0.01
	Mean change (days)	2.0 ± 0.13	3.6 ± 0.25	2.1 ± 0.08	1.0 ± 0.31	5.9 ± 0.28	4.1 ± 0.13	6.5 ± 0.11
	ΔP 90th percentile	1.4 ± 0.03	1.9 ± 0.07	1.5 ± 0.04	1.4 ± 0.10	2.6 ± 0.11	1.8 ± 0.03	2.5 ± 0.06
	Mean change (days)	2.0 ± 0.20	3.6 ± 0.28	2.0 ± 0.16	0.9 ± 0.36	5.7 ± 0.35	3.8 ± 0.16	6.0 ± 0.18
First decile	ΔP mean	1.0 ± 0.01	1.0 ± 0.01	1.0 ± 0.01	1.1 ± 0.02	1.1 ± 0.02	1.0 ± 0.01	1.2 ± 0.02
Total rain	Mean change (mm)	0.1 ± 0.03	*0.1* ± 0.06	−0.1 ± 0.03	0.5 ± 0.18	0.7 ± 0.13	0.2 ± 0.06	1.0 ± 0.12
Tenth decile	ΔP mean	0.9 ± 0.01	0.9 ± 0.01	1.0 ± 0.01	1.0 ± 0.02	0.8 ± 0.02	0.9 ± 0.01	0.8 ± 0.02
Total rain	Mean change (mm)	−12.1 ± 0.97	−10.9 ± 1.33	*1.2* ± 2.00	*−1.8* ± 2.17	−44.4 ± 3.72	−25.7 ± 2.44	−52.5 ± 5.75
Tenth decile	ΔP mean	1.0 ± 0.01	1.1 ± 0.01	1.1 ± 0.01	1.0 ± 0.01	1.0 ± 0.01	1.0 ± 0.01	1.1 ± 0.02
Rain per day	Mean change (mm day^{-1})	0.4 ± 0.04	0.9 ± 0.03	0.9 ± 0.13	0.1 ± 0.03	0.3 ± 0.07	0.5 ± 0.09	0.6 ± 0.09
*n*_days	ΔP mean	0.8 ± 0.01	0.8 ± 0.01	0.8 ± 0.01	0.8 ± 0.02	0.7 ± 0.02	0.8 ± 0.01	0.6 ± 0.01
	Mean change (days)	−0.6 ± 0.04	−0.9 ± 0.09	−0.6 ± 0.04	−1.9 ± 0.46	−2.6 ± 0.21	−1.1 ± 0.13	−4.9 ± 0.29
intens	ΔP mean	1.0 ± 0.01	1.1 ± 0.01	1.1 ± 0.01	1.0 ± 0.02	1.1 ± 0.02	1.1 ± 0.01	1.1 ± 0.02
	Mean change (mm day^{-1})	0.4 ± 0.12	0.9 ± 0.10	2.2 ± 0.20	0.1 ± 0.04	0.7 ± 0.14	1.3 ± 0.21	1.4 ± 0.2

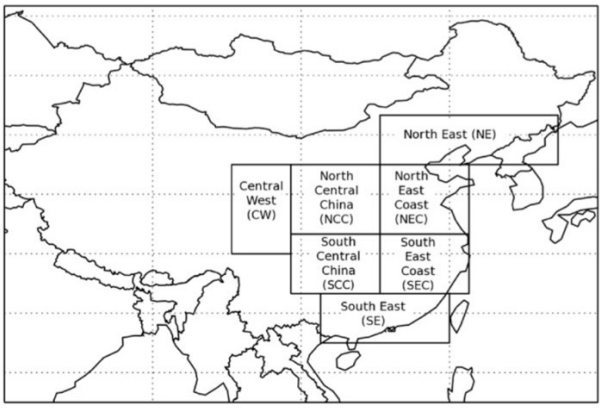

Figure 2 Divided areas in China (Burke and Scott 2017)

Scott built a model by analyzing mean, mean changes and 10th percentile mean changes in total rainfall, mean, mean changes and 90th percentile mean changes in dry days, mean and mean changes in the first decile and tenth decile of total rainfall, and also intensity in past 65 years (Burke and Scott 2017). While changes are different in the regions, for the entire domain the total precipitation is decreasing and the number of dry days is increasing. Data in the first decile and tenth decile of total rainfall shows onset of the rainy season occurring later, duration of rainy season is decreasing, but the occurrence of heavy rain events is increasing (Burke and Scott 2017). These are strong evidence of anthropic climate change is making an impact on EASM and changes are varied in regions.

Normally, less rainfall is associated with less cloudiness. The previous research shows a decreasing annual mean total cloud amounts from 1961 to 2000 by using data from 466 meteorological stations over China mainland (Ding et al. 2017). Figure 3 shows a reducing trend of total cloud amount from 1961 to 2000 in China (Ding et al. 2017). With less precipitation and less cloudiness, incoming solar irradiance is supposed to increase without counting other influence such as fog and haze weather.

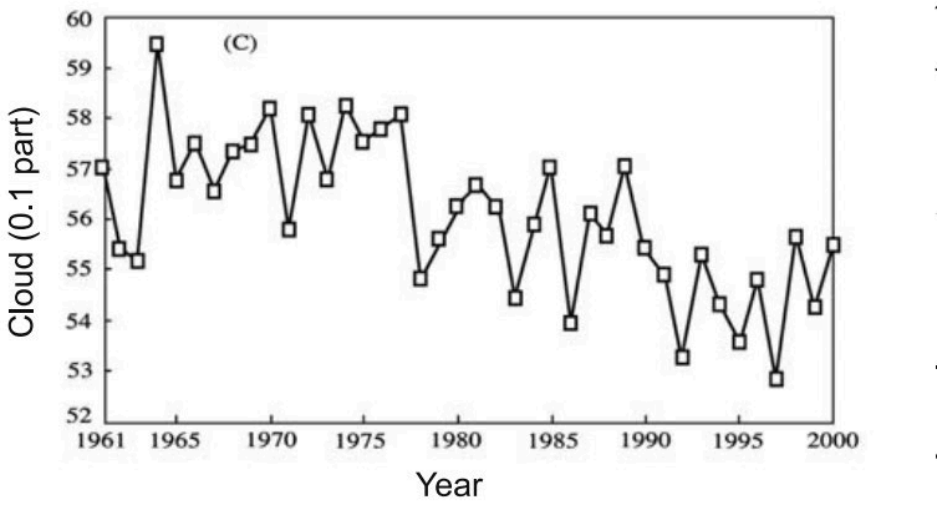

Figure 3 Annual Mean of Total Cloud Amount in China

The connection between the use of traditional power resources like coal, gas, and oil to increasing aerosol and greenhouse emissions and subsequent global warming is will established. More countries have started making policies and plans toward switching from traditional power resource to renewable power resource like wind, water and solar. In developing countries like China, it requires more energy resources to establish and to develop with less pollution; the government is making policies toward supporting solar energy industries and building solar farms. This includes the Tibetan Plateau which has such rich solar power resource. According to IEA, China is the largest manufacturer of solar panel technology, and 60% of the world 's solar

panels are made in China (Baraniuk 2018). Figure 4 shows the current locations of solar farms, which is the guide map used to analyze surface incoming solar irradiance on specific locations.

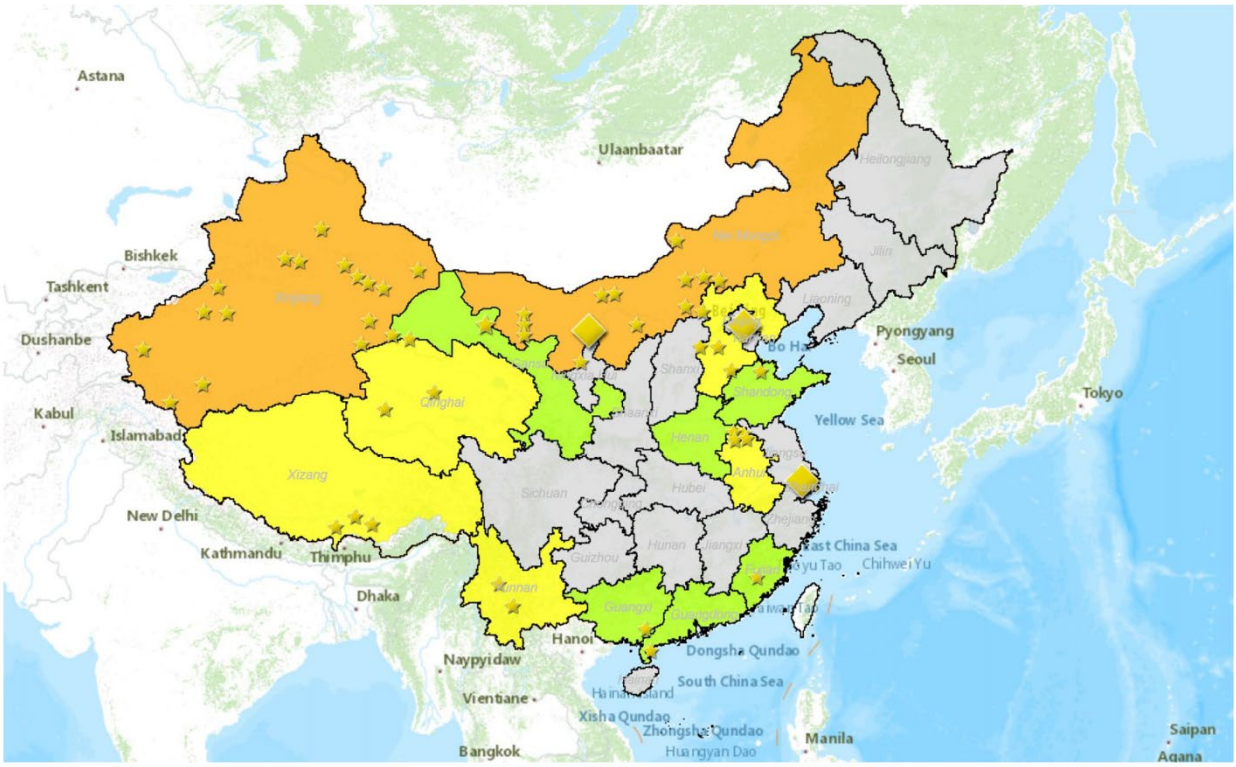

Figure 4 Solar Farms Map in China (Stars mean the single location has one solar farm and Squares mean the single location has more than one solar farms) (Data source from ArcGIS)

In China, not only changes in atmospheric circulation may make changes in cloud cover and solar radiation, events like haze and fog also affect cloud cover and solar radiation. The latter are closely related to the growing amount of aerosol emissions with rapidly increasing development. Figure 5 shows an increase in the number of days with haze and fog weather (related to pollution), which make an impact on the availability of solar energy in specific areas, in China from 1981 to 2010(You et al. 2018). Increasing fog and haze weather brought more cloud cover in China, and cloud nuclei was increased due to pollution. More cloud nuclei created

by pollution would lead an increase in cloud solar radiance reflection (Twomey 1974).

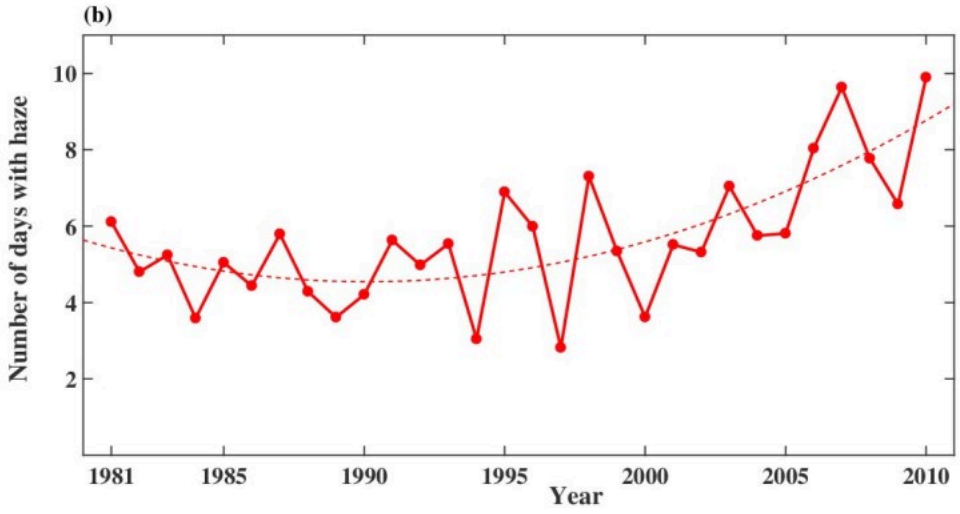

Figure 5 Number of days with haze and fog weather in China (You et al. 2018)

Increasing solar radiance reflection by clouds eventually decrease surface incoming solar irradiance, which would affect the capacity of solar energy collection. Figure 6 is an average air pollution map in China, which contains data of PM2.5, PM 10 and ozone. The map shows a clearly evidence that most air pollution is concentrated in eastern and southern China where most mega cities are located. This same area would experience a decline in solar irradiance, since more PM2.5, PM 10 and ozone emission would lead to an increase in haze and fog weather.

This research uses solar irradiance data between 1980 to 2017 from NASA Merra-2 data set to analyze the change brought by both natural-caused and human-caused factors. A comparison is made with data from previous papers which analyze changes in the EASM and haze and fog weather to examine the anthropic impact on the capacity of solar energy collection.

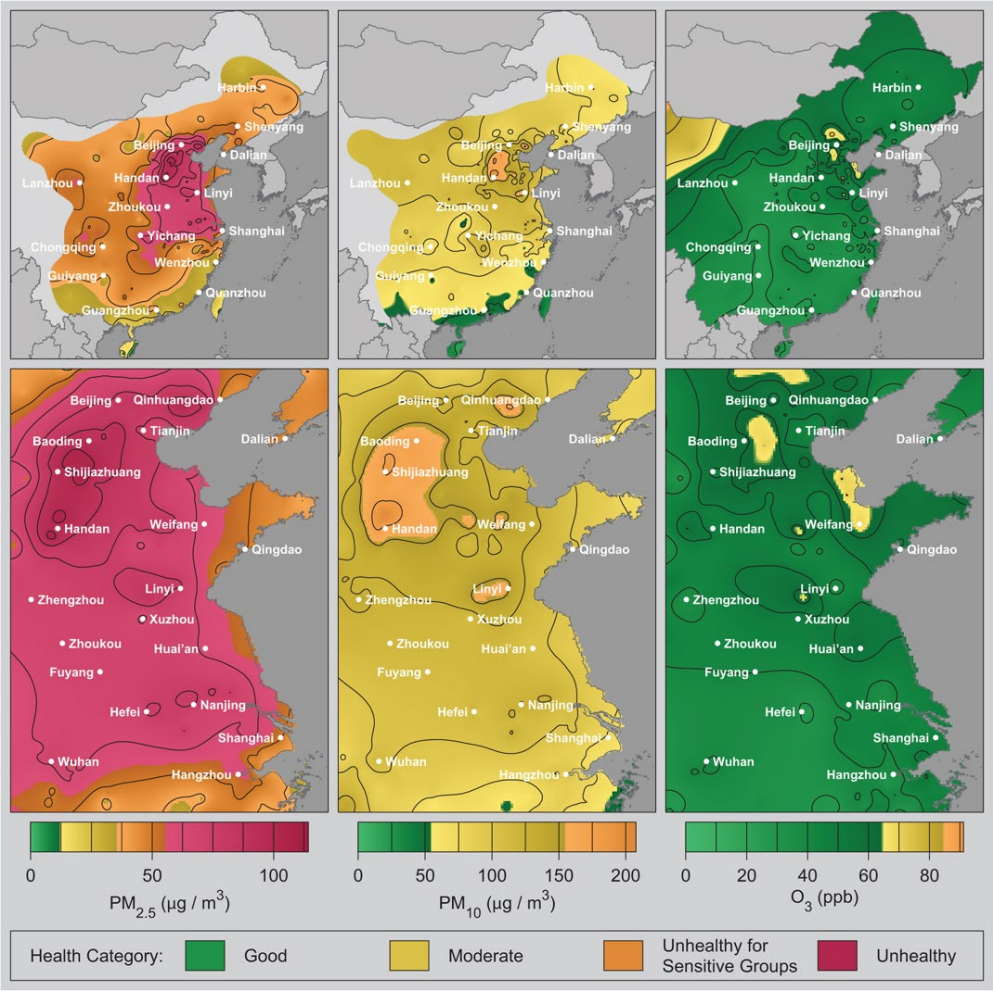

Figure 6 Average air pollution maps in China (Rohde and Muller 2015)

CHAPTER II

METHODS

This research used data from NASA Modern-Era Retrospective Analysis for Research and Applications, Version 2 (MERRA-2) data set which provides data since 1980 (NASA 2019). Due to its improvement in assimilating GPS-RADIO occultation and modern hyperspectral radiance and microwave observation, it has replaced the original MERRA data set (NASA 2019). The dataset contains both GEOS model and the GSI assimilation model. Specifically, this research utilized shortwave radiation arriving at the surface over the China mainland and part of East Asia.

The MERRA-2 data set contains monthly means surface albedo for visible beam with different variables and has a one-hour temporal resolution, and a 0.5° times 0.625° spatial resolution. This research used the shortwave radiation data that had total net downward shortwaves flux which contained, non-clear sky, clear sky and no aerosol. The data format is netCDF, and this research used MATLAB for the entire analysis process, which is a software and programming language built by MathWorks that helps to express matrix and array mathematics directly (MATLAB 2019). The data is in three dimensions of latitude, longitude and time. Latitude had a range between 15 degrees and 60 degrees North with 100 variables; longitude had a range between 73 degrees and 135 degrees East 91 variables and time had a range between year 1980 to 2017 with 456 variables. This research divided the data into four nearly decadal groups, first is from 1980 to 1991, second is from 1992 to 2000, third is from 2001 to 2010, and the last group is from 2011 to 2017.

The generated maps have the same latitude and longitude ranges which are 15 to 60 degrees North and 73 to 135 degrees East, and a color bar scale from red (high radiation) to blue (low radiation). The solar radiation unit is W/m^2 with a range from 30 to 300, and the maps show a five-interval difference. Comparison between four decades maps shows the change of solar radiation in regions visually. Other groups of maps were made by using the same method, but the data only contained the total net downward shortwaves flux with clear skies. Clear-sky data were also divided into four decades and created maps with same color bar and interval. Comparison between total solar radiation maps and clear-sky maps showed the influence of clouds. Another four maps were created to show total net downward shortwaves in regions, which included Southeastern, Northeastern, Southwestern and Northwestern parts in China. This research also grouped the solar radiation data by province. The plots showed trend lines which represent the change of solar radiation in specific locations which helps to identify the climate change and anthropic emission impact on the solar energy industry.

This research also created plots that show the trend of the annual mean of solar radiation of each province in China since 1980 to 2017, and compared it with haze and fog weather days trends. PM2.5 data trends were also compared and helped to identify the anthropic impact on the capacity of solar energy collection in China. The analyzed results of this research can also help with picking locations of future solar farms and predict the change of solar radiation in China in the future.

CHAPTER III

RESULTS

Figure 7 shows surface incoming solar radiation in China from the year 1980 to 1991. The Tibet Plateau still had a large amount of solar radiation. Most provinces in China had a solar irradiance range from 150 to 170 W/m^2. The solar irradiance in a small area of Shanxi province reached a range between 170 to 180 W/m^2. The most area in Guizhou, Guangdong, and Fujian had solar radiation at least 170 and up to over 185 W/m^2.

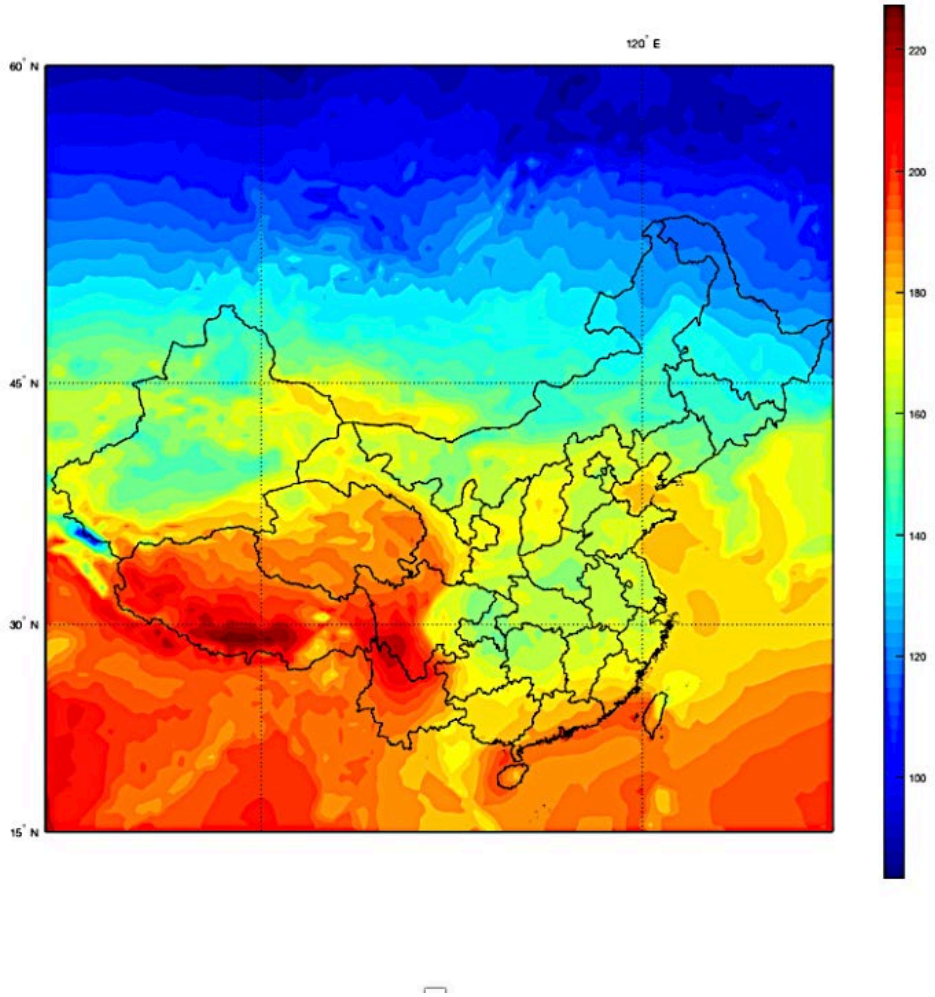

Figure 7 Surface Incoming Solar Radiation 1980-1991

Figure 8 shows surface incoming solar radiation in China from 1992 to 2000. The amount of solar radiation in Tibet Plateau does not change appreciably. The solar radiation in the area of northwestern Qinghai had decreased, some area experienced a change between 5 to 10 W/m^2. Compared to figure 7, the high solar irradiance area in Shanxi had surprisingly expanded. The solar irradiance in Eastern Xinjiang had decreased. The most apparent change was found in southern China which contains Guizhou, Guangxi, Guangdong, and Fujian, the most areas had solar irradiance around 170 W/m^2, and the only small area had reached to closer 180 W/m^2.The same area between 1980 to 1991 had solar irradiance mostly around 180 W/m^2, and the top area had reached 185 W/m^2. The rest of the province did not change much, and most areas in eastern China had incoming solar radiation around 160 and up to 170 W/m^2.

Figure 9 shows surface incoming solar radiation in China from 2001 to 2010. Compared to figure 7 and figure 8, the solar radiance on Tibet Plateau had no significant change. The solar irradiance in North and center of Qinghai were keeping decreasing. The high solar irradiance area in Shanxi also experienced a loss of solar energy between 2001 to 2010. The most regions of Guizhou, Guangxi, Guangdong, and Fujian had an average incoming solar irradiance of 170 W/m^2. Most provinces in Eastern China were losing solar energy between the year 1992 to 2010 with a declined change of 5 to 10 W/m^2.

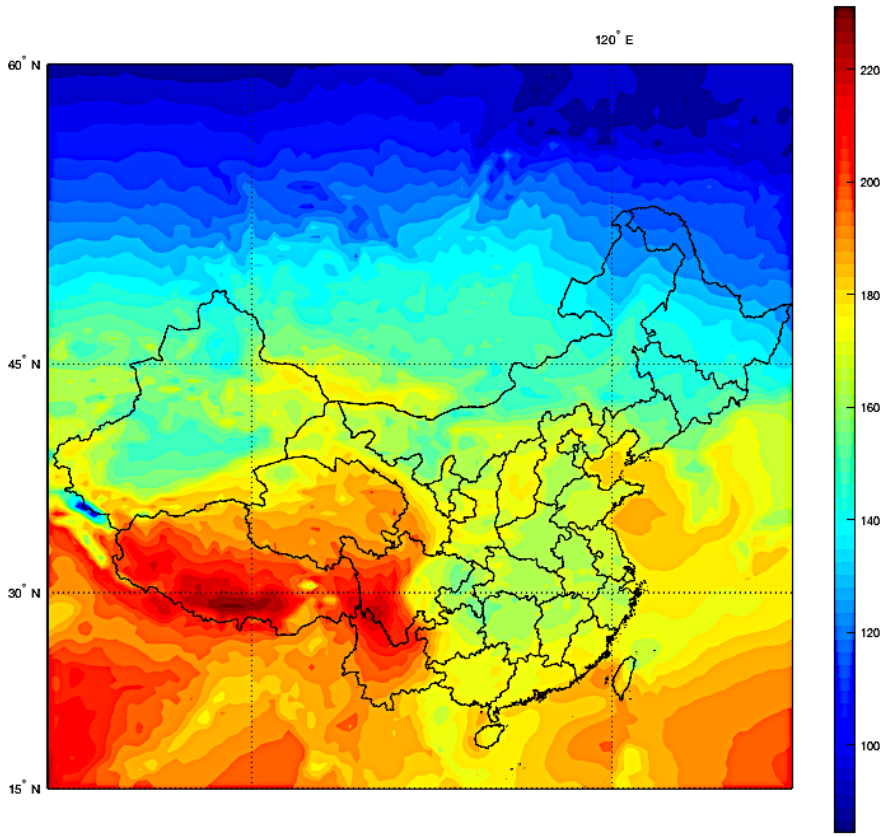

Figure 8 Surface Incoming Solar Radiation 1992-2000

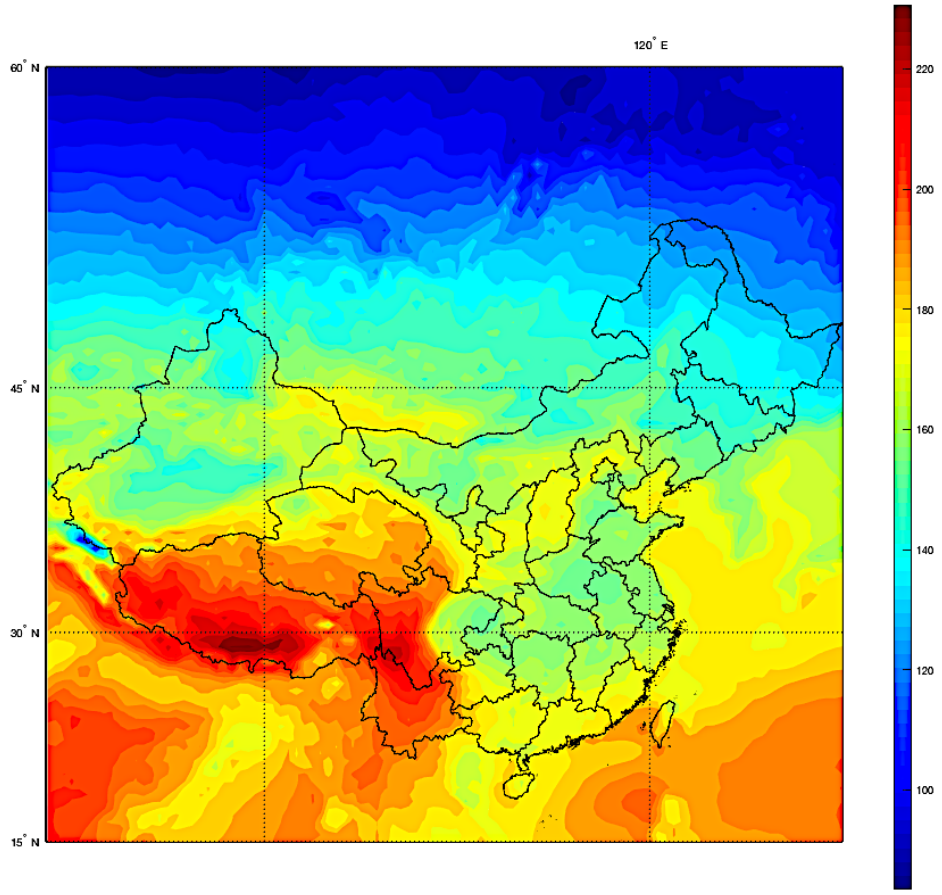

Figure 9 Surface Incoming Solar Radiation 2001-2010

Figure 10 shows Surface incoming solar radiation in China between the year 2011 to 2017. Compared to previous figures, most areas of the Tibet Plateau had stable solar radiation in the last 40 years. Only parts of territory along the border line between China and India experienced loss in solar irradiance from 170 to around 155 W/m^2. The north and central area of Qinghai, which keeps the loss of solar irradiance in 20 years, experienced an increase between the year 2011 to 2017. Over 99% of Shani province were received solar irradiance around 170 W/m^2. The whole east of China continued to lose solar energy during this period. The regions in southern China were getting less solar power with only a few areas receiving 170 W/m^2.

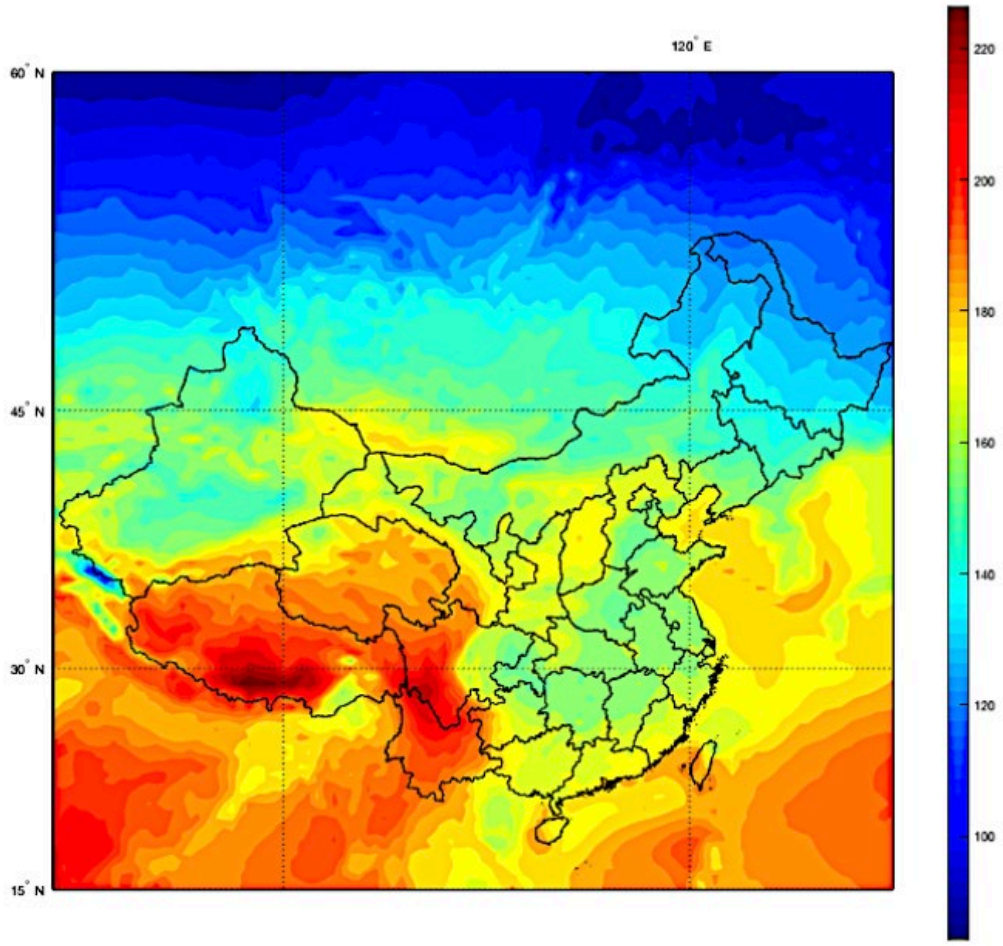

Figure 10 Surface Incoming Solar Radiation 2011-2017

Figure 11 shows four decadal average of surface incoming solar radiation with clear sky and no aerosols. Comparing these four panels, we find no remarkable changes in incoming solar radiation on most parts of China mainland. But incoming solar irradiance did increase by nearly 25 W/m^2 in western Sichuan, north of Hubei, Anhui and Jiangsu provinces.

Figure 12 shows the plot for surface incoming solar radiation from 1980 to 2017 in Guangdong province which has one large solar farm. Figure 13 shows the plot of surface incoming solar radiation from 1980 to 2017 in Henan province which is in middle-east of China and has one large solar farm. Both plots show the evidences of surface incoming radiation's

decline in China, specifically in the east of China where most developed cities are located, and pollutants are produced. Surface incoming solar radiation in Guangdong experienced up and down in last forty years, but with an average over 15 W/m^2decrease. Surface incoming solar radiation in Henan experienced the decreasing in an average over 10 W/m^2. In fact, the incoming solar radiation in Henan had a remarkable decrease after 1997. Figure A1 to A32 shows the plots for surface incoming radiation from 1980 to 2017 in other provinces.

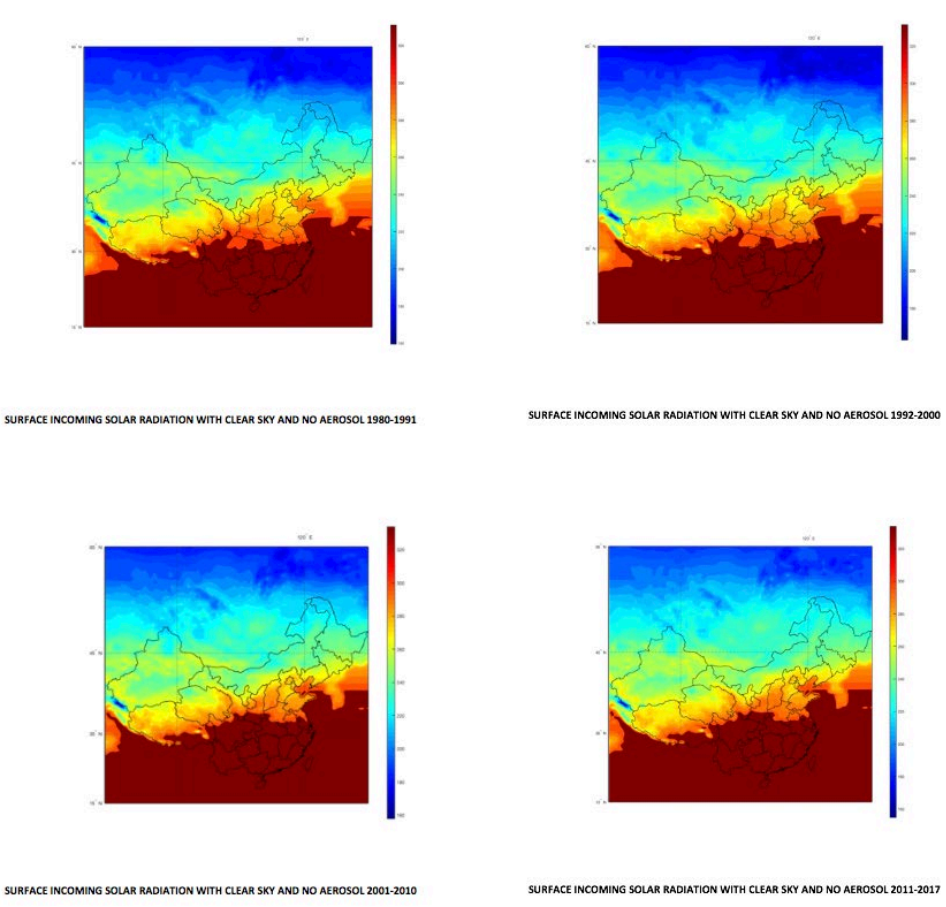

Figure 11 Surface Incoming Solar Radiation with Clear Sky and No Aerosol

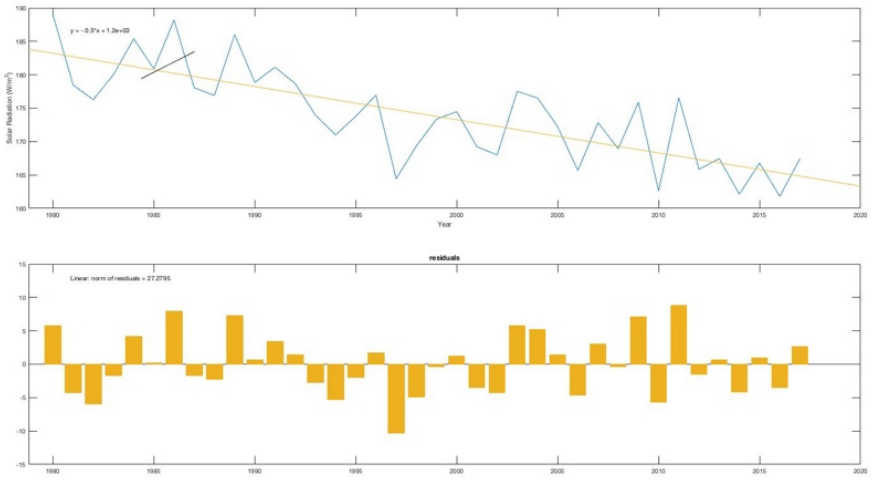

Figure 12 Guangdong Surface Incoming Solar Radiation 1980-2017

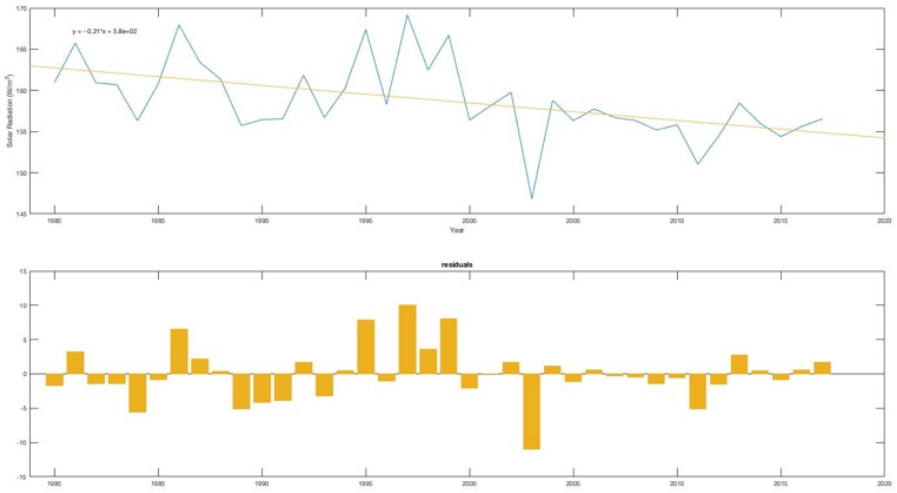

Figure 13 Henan Surface Incoming Solar Radiation 1980-2017

CHAPTER IV

DISCUSSION

China has a land area of over 9.6 million square kilometers and the highest plateau in the world, the Tibet plateau, which lead to a large amount of solar energy capacity in China. As the global society is making efforts towards building on a "greener" society that relies on more renewable energy instead of consuming fossil and coal, the solar resource in China can provide more electricity and support reducing aerosol and greenhouse emission. The Tibet Plateau is described as the roof of the world, not only due to its high average altitude, but also due to its rich natural resources like water and sola. Although the precipitation and cloud cover have likely been affected by climate change, the Tibet Plateau is still the area contains an extremely high amount of solar energy. Figure 14 is the map made by analyzing solar irradiance data from NASA and shows surface incoming solar radiation in China from 1980 to 2017. It has a color bar from low solar irradiation which is the cold blue color to high solar irradiation which is a warm red color and units in W/m^2. The area of Tibet Plateau contains the west part of Sichuan province, southern Qinghai Province and all Xizang autonomous region shows that it received higher average solar irradiance compared to other areas, which represents the area has an average incoming solar radiation range from 180 to 220 W/m^2 in the last forty years. As the results showing in figure 3 which are the locations of large solar farms in China, there are only five solar farms in this area. It could be that the difficulty of building solar installations in high altitude area and the high cost of transport the electricity to developed cities located in Eastern China have limited solar production on the Tibetan Plateau, which is the area that consumes and

need more electricity. However, it is still possible for building solar farms in an area without extreme high altitude on Tibet Plateau and finding a way to use the rich solar resource in that area effectively for the larger population areas to the East. Provinces like Shanxi, Guizhou, Guangdong, and Guangxi also have the capacity of collecting solar power with a range between 160 and 170 W/m^2. Those are all possible locations for building higher efficiency solar farms.

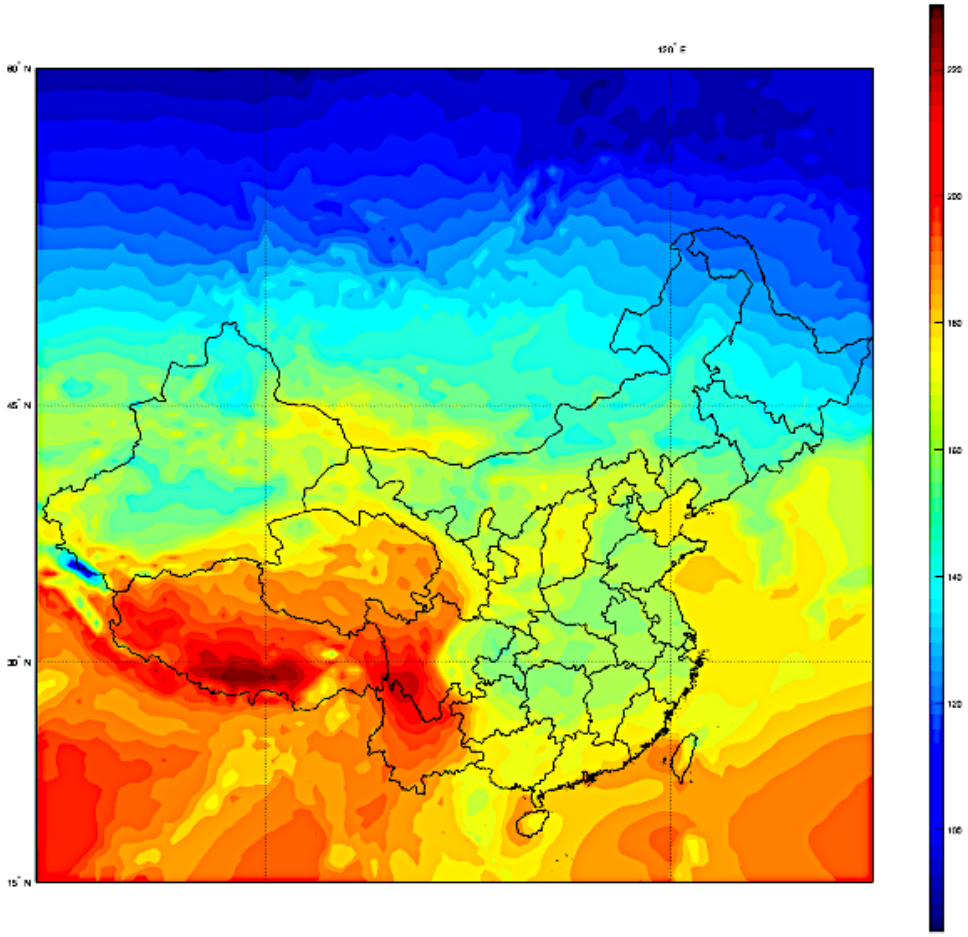

Figure 14 Surface Incoming Solar Radiation 1980-2017

Shanxi, an area with receiving stable solar irradiance around 170 W/m^2in the last forty years, does not have a single large solar farm. This province should be considered as the next target place to build solar farms in order to develop and collect solar energy. The same situation has founded in Yunnan, an area with receiving an average solar irradiance over 170 W/m^2 in the last forty years, only had two large solar farms. It also could be another target area for building solar farms. Compared Shani and Yunnan provinces, both had received a stable solar irradiance with no significant change. Shanxi has a lower amount of solar irradiance, but its location is closer to the other developed area in East China which will reduce the cost of transporting electricity. Yunnan had received at least a monthly average 10 W/m^2 more on solar irradiance in last forty years, but due to its geographical location, it would cost more to transfer electricity from there to eastern China.

Comparing the average incoming solar irradiance maps and the average air pollution map of China, areas that experienced more decline in incoming solar irradiance was similar with the areas that experienced more air pollution. These areas also had more haze and fog weather in last forty years due to air pollution, which could be the primary cause of changes on incoming solar irradiance. Previous research also identified global warming was making effects on EASM with change in precipitation and extreme weather events (Burke and Scott 2017). Changes in precipitation and extreme weather events brought changes in cloud cover, which also could be the possible cause of change on incoming solar irradiance.

CHAPTER V

CONCLUSION

As the results showed in this research, the changes in incoming surface solar irradiance have been identified in China over the last 40 years. First of all, results showed the incoming solar irradiance remained at a stable level in the Tibet Plateau area with a large amount of solar energy capacity. In this region, only the small area along the boundary line between China and India showed a decrease by 10 W/m^2, which is about 6.25% overall. Qinghai, a province receives rich solar energy, which has its south part on Tibet Plateau, has lost 5 to 10 W/m^2 on its incoming solar irradiance over the last 40 years. Xinjiang, another province with more than ten large solar farms built in, had kept received a stable amount of solar energy, with only a small area experienced decreasing of 10 W/m^2 in Eastern Xinjiang along the boundary line between China and Mongolia. Neimenggu, a province also contains more than ten large solar farms, also kept received solar energy at a stable level, but the amount of solar irradiance was between 150 to 165 W/m^2 which is quite low compared to Xinjiang, Qinghai and Xizang.

The provinces in southern China, which include Guizhou, Guangxi, Guangdong, and Fujian, experienced a drop of 10 to 15 W/m^2 of incoming solar irradiance in the last forty years. These are the provinces with more factories and higher population density, compared to the other provinces in China. Increased aerosol emission that caused haze and fog weather could be the reason for the drop of solar irradiance. The change of rainy season and increased extreme precipitation event also can affect the ability to receive solar energy in that area. The most important finding of this research is most areas in Eastern China which are the most developed area and experienced the most haze and fog weather had lost their incoming solar irradiance on

the surface on an average between 15 to 20 W/m^2, which is about 10-15% overall in last forty years.

The marked decrease in surface solar irradiance in eastern and southern provinces documented in this research corresponds well to the pollution distribution described by Figure 5. The total downward irradiance with clear sky and no aerosol did not have a remarkable change through forty years. The impact of climate change, through the mechanism of EASM rainy season onset and duration (Li et al. 2010) and (Ding et al. 2007) would suggest less cloud amount associated with the observed reduction in rainfall. This would suggest that the climate change contribution via cloud amount may actually work to increase solar availability. Taken together, this research suggests that the dominant source of the "dimming" seen in the MERRA-2 dataset in the most affected provinces is related to the increasing haze/fog weather as the result of direct emissions of pollutants in and upstream of these regions. Based on the analysis so far, we speculate that a combination of EASM change and increasing haze weather lead to the overall decline in incoming solar irradiance over East Asia.

Future work will focus on how to separate the contributions from the large-scale weather and clouds versus the contributions from direct aerosol/pollutant emission on solar availability. Furthermore, whether the large-scale cloudiness can be attributed to a climate change signal such as the EASM should be explored. The possibility that climate change may actually increase solar energy capacity in areas less affected by air pollution, for example northeast and southwest China, is another topic for future exploration.

REFERENCES

Baraniuk, C., 2018: Future - How China's giant solar farms are transforming world energy. BBC News. http://www.bbc.com/future/story/20180822-why-china-is-transforming-the-worlds-solar-energy (Accessed January 28, 2019).

Burke, C., and P. Stott, 2017: Impact of Anthropogenic Climate Change on the East Asian Summer Monsoon. Journal of Climate, 30, 5205–5220, doi:10.1175/jcli-d-16-0892.1.

Ding, Y., and J. C. L. Chan, 2005: The East Asian summer monsoon: an overview. Meteorology and Atmospheric Physics, 89, 117–142, doi:10.1007/s00703-005-0125-z.

Ding, Y., G. Ren, Z. Zhao, Y. Xu, Y. Luo, Q. Li, and J. Zhang, 2007: Detection, causes and projection of climate change over China: An overview of recent progress. Advances in Atmospheric Sciences, 24, 954–971, doi:10.1007/s00376-007-0954-4.

Li, J., Z. Wu, Z. Jiang, and J. He, 2010: Can Global Warming Strengthen the East Asian Summer Monsoon? Journal of Climate, 23, 6696–6705, doi:10.1175/2010jcli3434.1.

MathWorks, 2019: MATLAB overview. Accessed 28 February2019, https://www.mathworks.com/products/matlab.html

NOAA, 2016: Climate Change Indicators U.S. and Global Precipitation. Accessed 10 January 2019, https://www.epa.gov/climate-indicators/climate-change-indicators-us-and-global-precipitation

NASA, 2017: Global Temperature. Accessed 10 January 2019, https://climate.nasa.gov/vital-signs/global-temperature/

NASA,2019: Modern-Era Retrospective analysis for Research and Applications, Version 2 , Accessed 28 February 2019, https://gmao.gsfc.nasa.gov/reanalysis/MERRA-2/

Rohde, R. A., and R. A. Muller, 2015: Air Pollution in China: Mapping of Concentrations and Sources. Plos One, 10, doi:10.1371/journal.pone.0135749.

Twomey, S., 1974: Pollution and the Planetary Albedo. Atmospheric Environment, 41, 120–125, doi:10.1016/j.atmosenv.2007.10.062.

Wang, B., Z. Wu, J. Li, J. Liu, C.-P. Chang, Y. Ding, and G. Wu, 2008: How to Measure the Strength of the East Asian Summer Monsoon. Journal of Climate, 21, 4449–4463, doi:10.1175/2008jcli2183.1.

You, Y., and Coauthors, 2018: Variations of Haze Pollution in China Modulated by Thermal Forcing of the Western Pacific Warm Pool. Atmosphere, 9, 314, doi:10.3390/atmos9080314.

APPENDIX

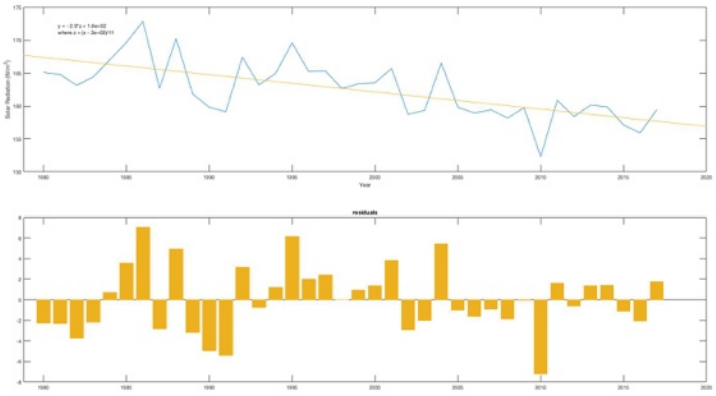

Figure A1 Anhui Surface Incoming Solar Radiation 1980-2017

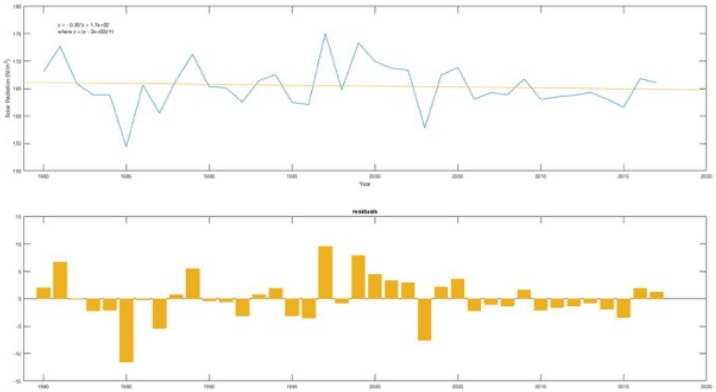

Figure A2 Beijing Surface Incoming Solar Radiation 1980-2017

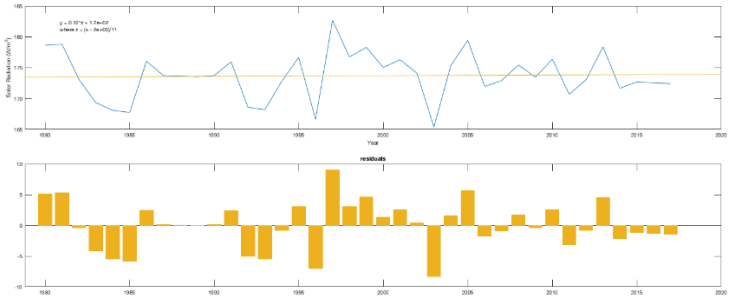

Figure A3 Shanxi (Jin) Surface Incoming Solar Radiation 1980-2017

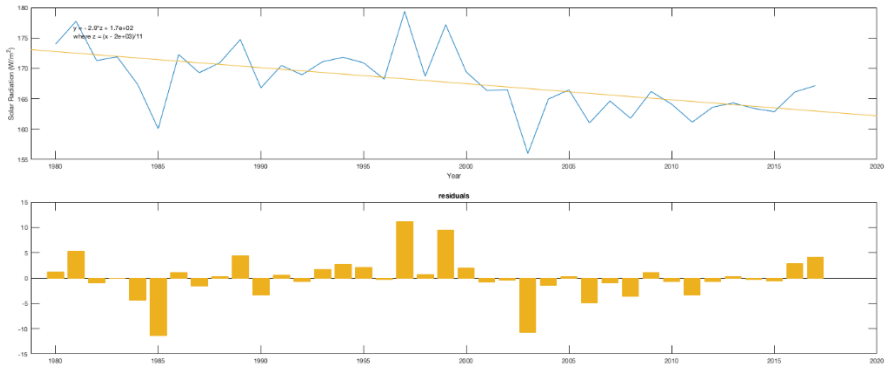

Figure A4 Tianjin Surface Incoming Solar Radiation 1980-2017

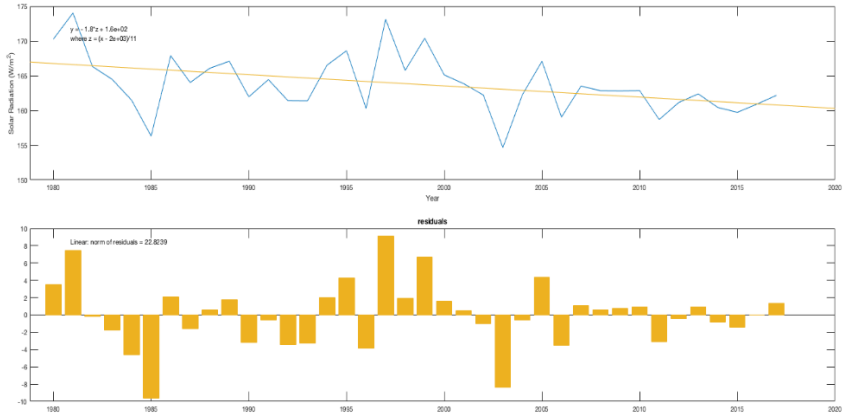

Figure A5 Hebei Surface Incoming Solar Radiation 1980-2017

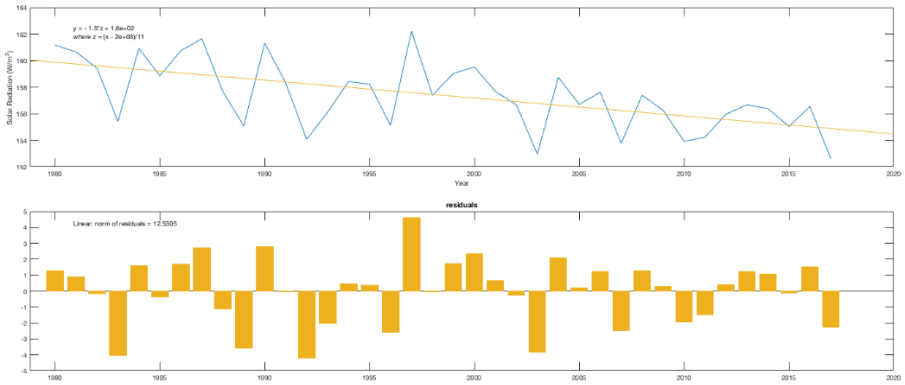

Figure A6 Neimenggu Surface Incoming Solar Radiation 1980-2017

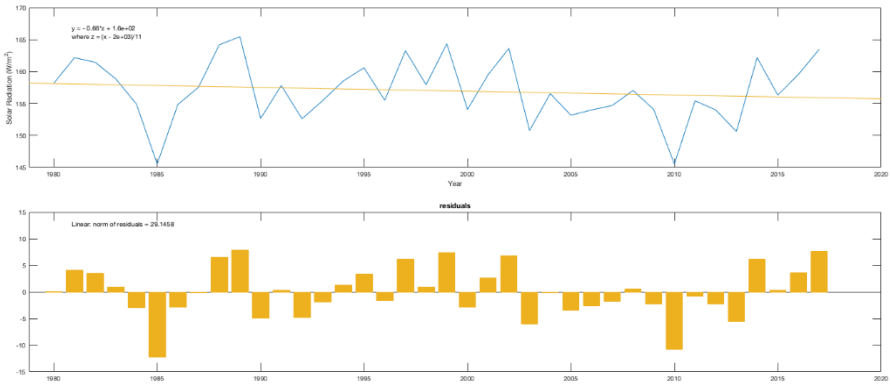

Figure A7 Liaoning Surface Incoming Solar Radiation 1980-2017

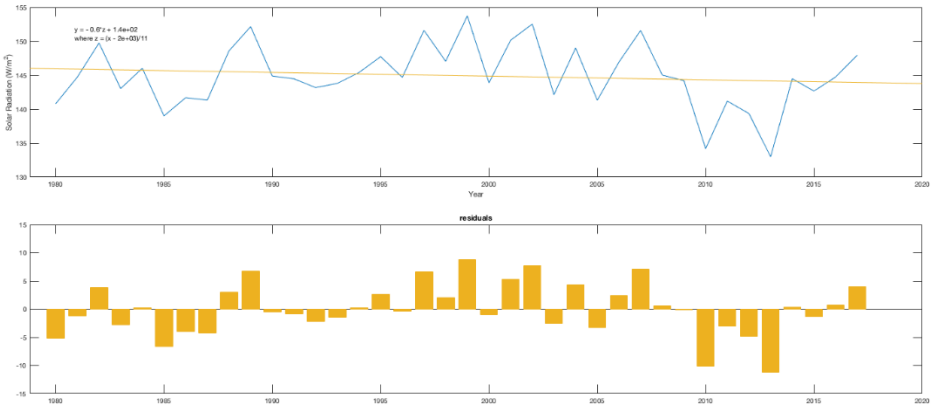

Figure A8 Jilin Surface Incoming Solar Radiation 1980-2017

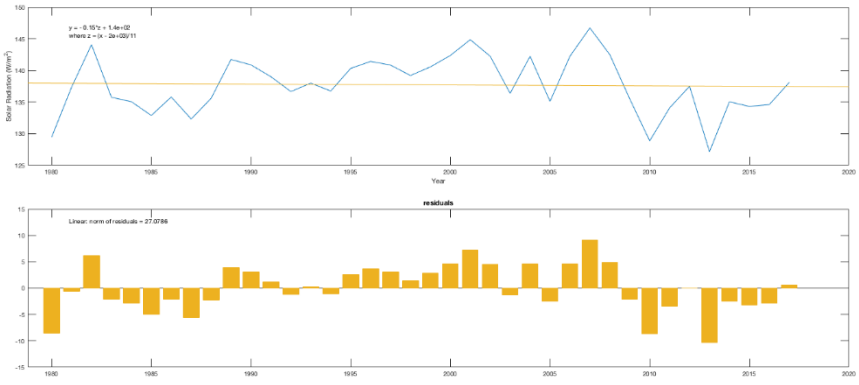

Figure A9 Heilongjiang Surface Incoming Solar Radiation 1980-2017

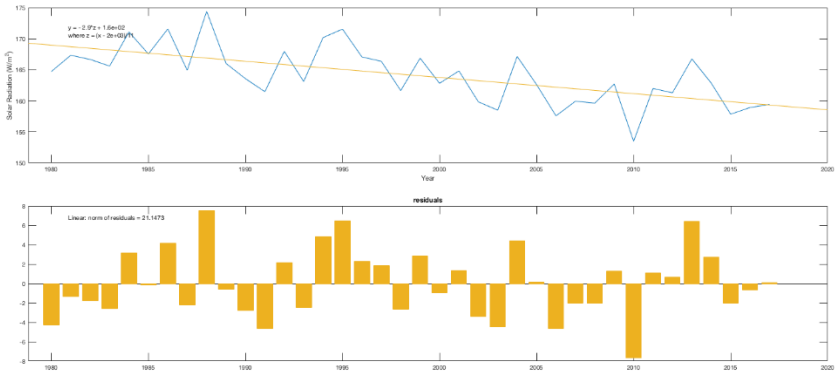

Figure A10 Shanghai Surface Incoming Solar Radiation 1980-2017

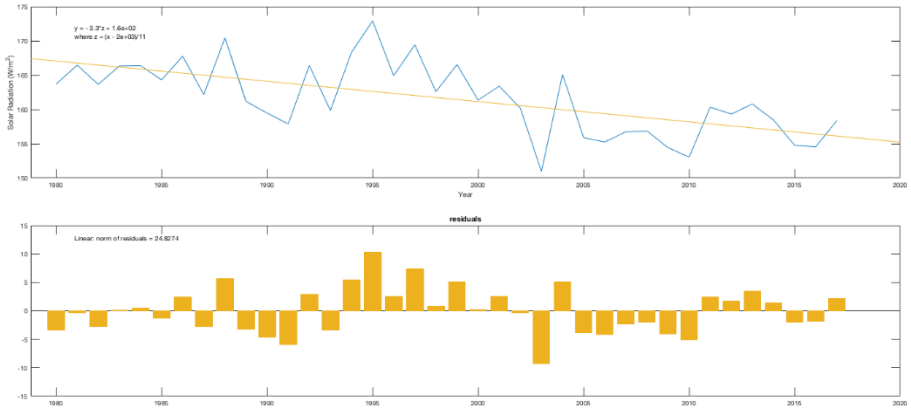

Figure A11 Jiangsu Surface Incoming Solar Radiation 1980-2017

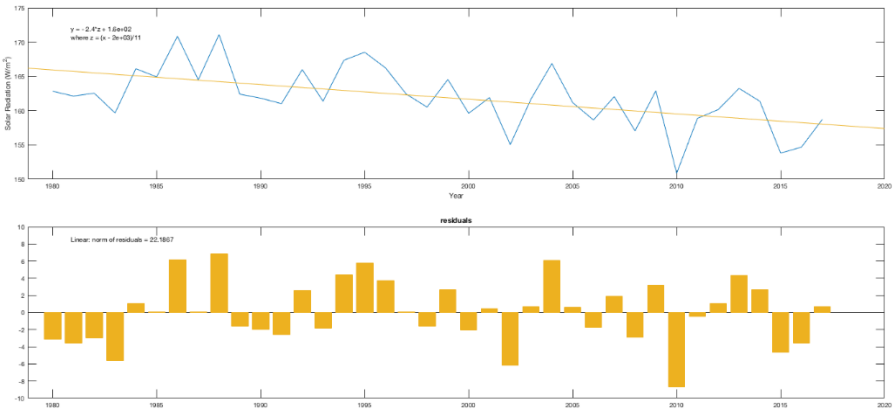

Figure A12 Zhejiang Surface Incoming Solar Radiation 1980-2017

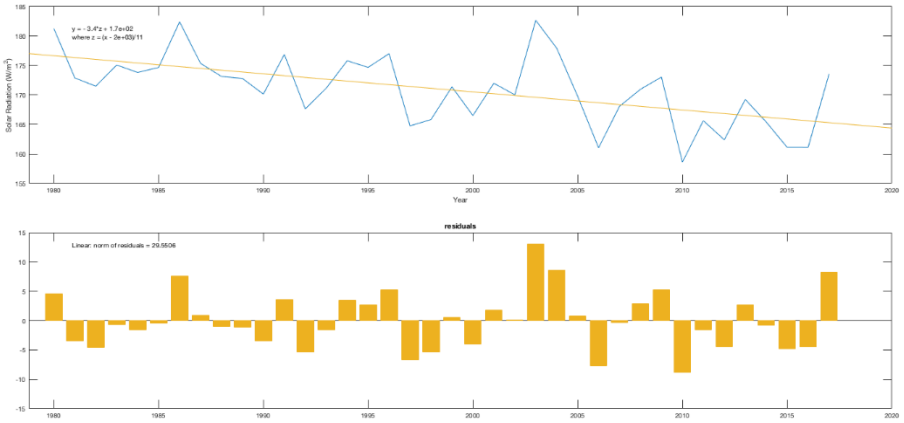

Figure A13 Fujian Surface Incoming Solar Radiation 1980-2017

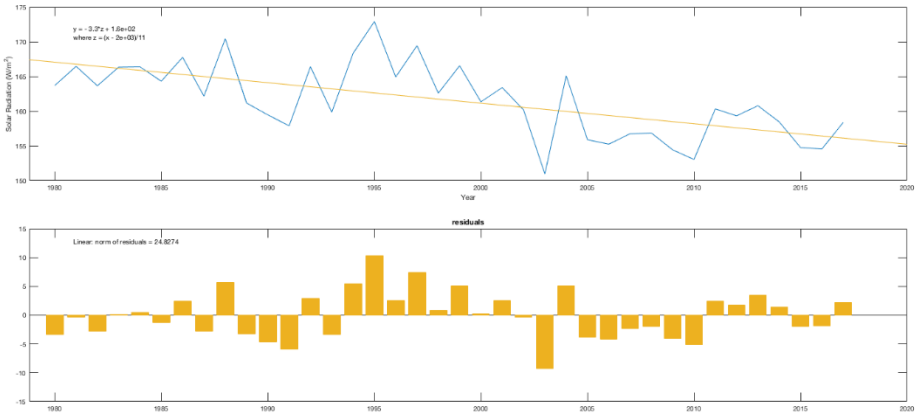

Figure A14 Jiangxi Surface Incoming Solar Radiation 1980-2017

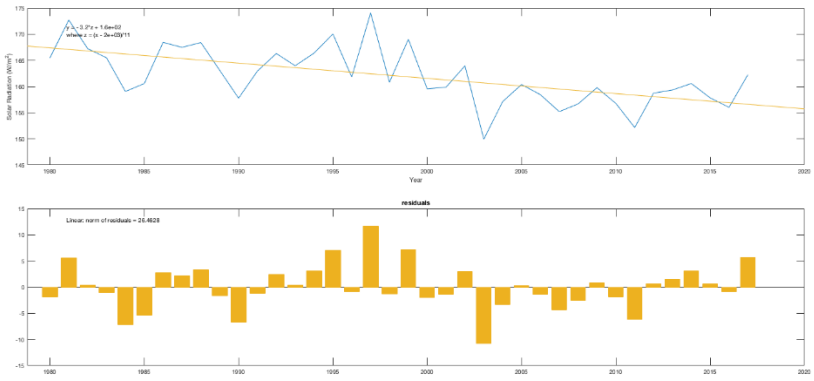

Figure A15 Shandong Surface Incoming Solar Radiation 1980-2017

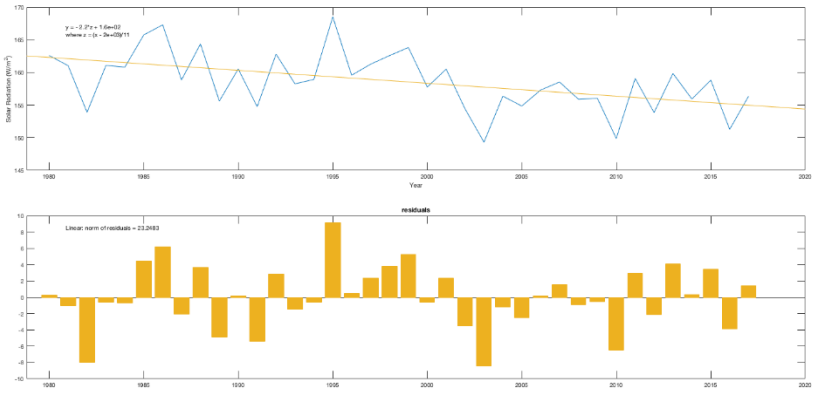

Figure A16 Hubei Surface Incoming Solar Radiation 1980-2017

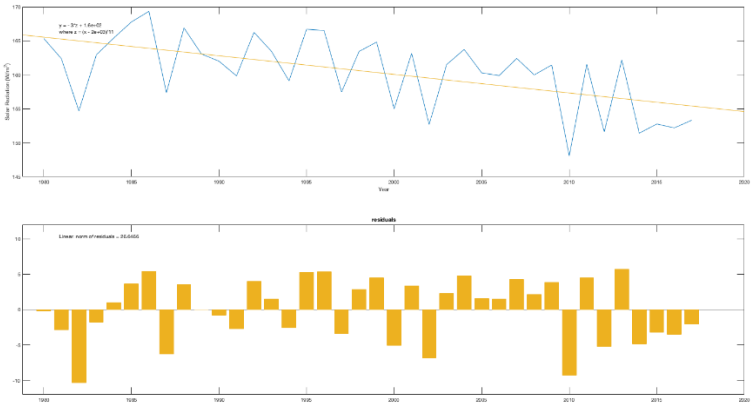

Figure A17 Hunan Surface Incoming Solar Radiation 1980-2017

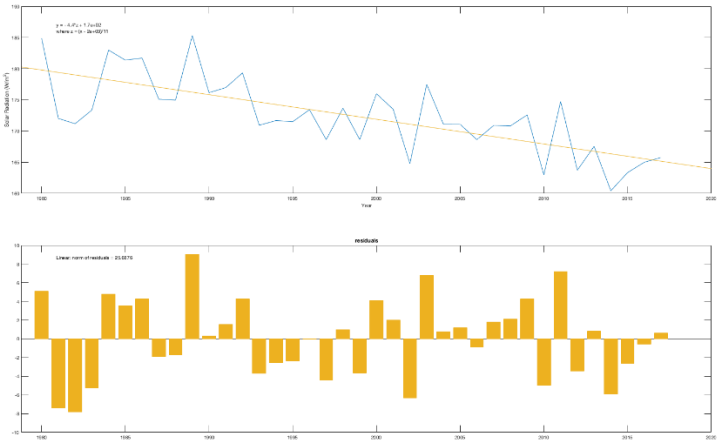

Figure A18 Guangxi Surface Incoming Solar Radiation 1980-2017

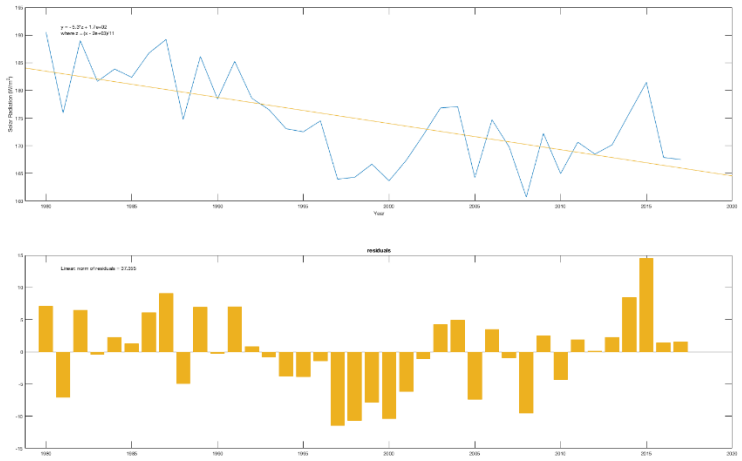

Figure A19 Hainan Surface Incoming Solar Radiation 1980-2017

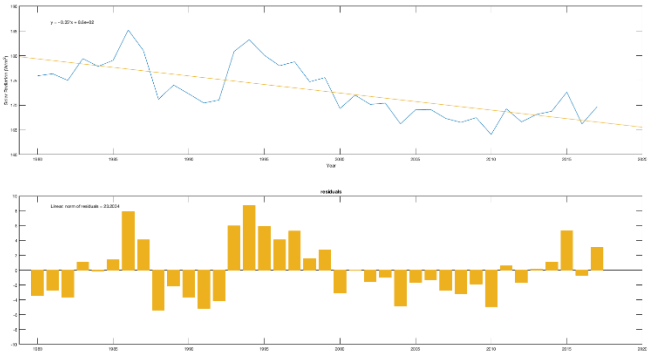

Figure A20 Sichuan Surface Incoming Solar Radiation 1980-2017

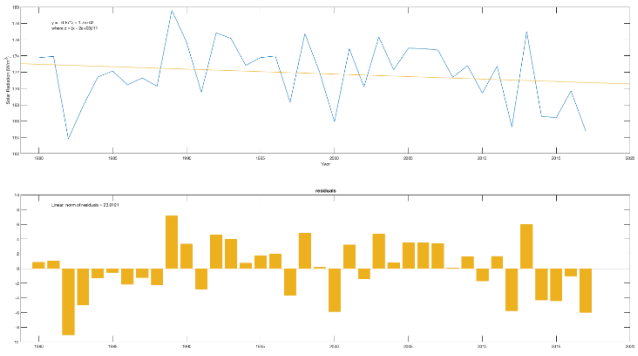

Figure A21 Guizhou Surface Incoming Solar Radiation 1980-2017

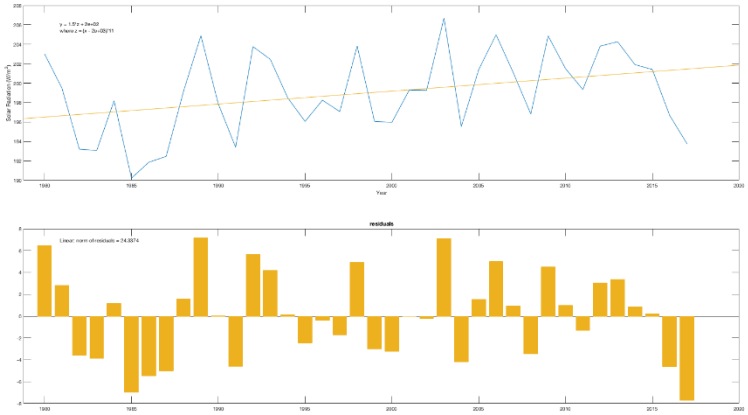

Figure A22 Yunnan Surface Incoming Solar Radiation 1980-2017

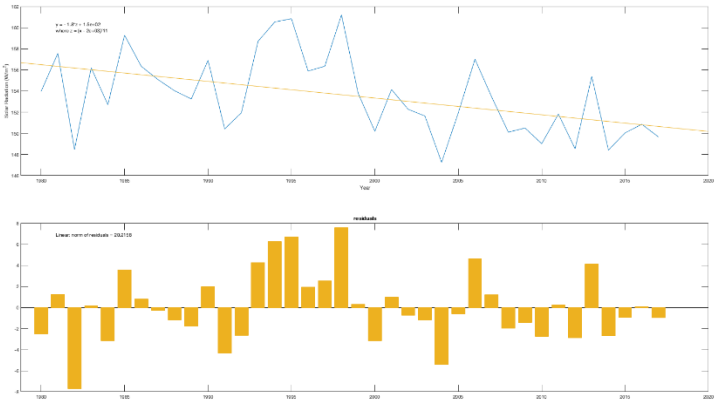

Figure A23 Chongqing Surface Incoming Solar Radiation 1980-2017

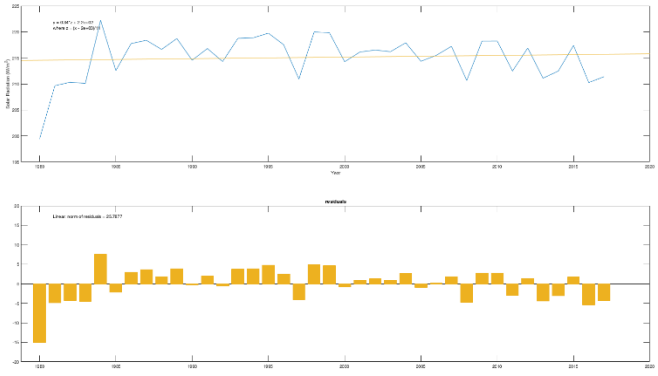

Figure A24 Xizang Surface Incoming Solar Radiation 1980-2017

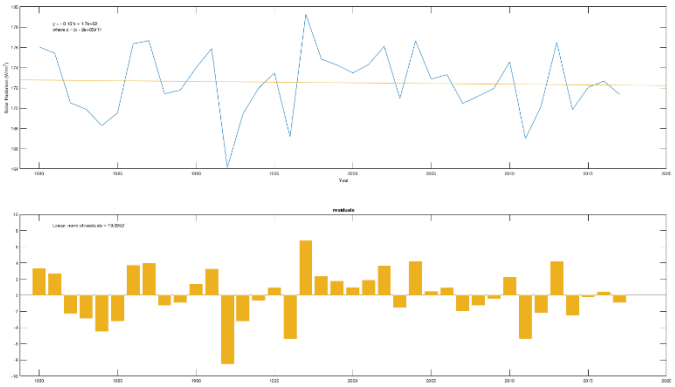

Figure A25 Shanxi (Shan) Surface Incoming Solar Radiation 1980-2017

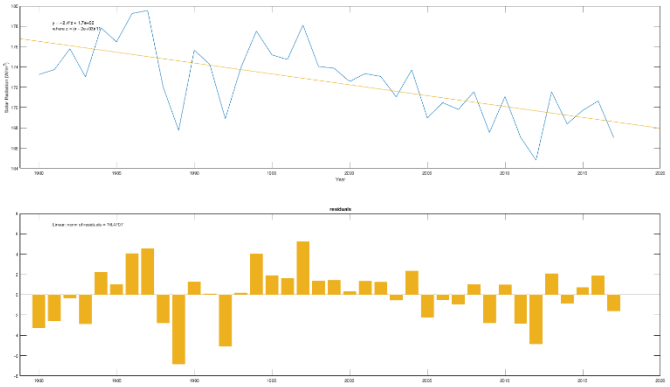

Figure A26 Gansu Surface Incoming Solar Radiation 1980-2017

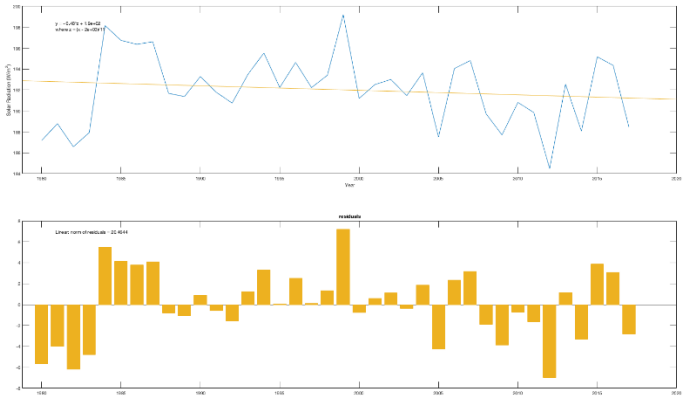

Figure A27 Qinghai Surface Incoming Solar Radiation 1980-2017

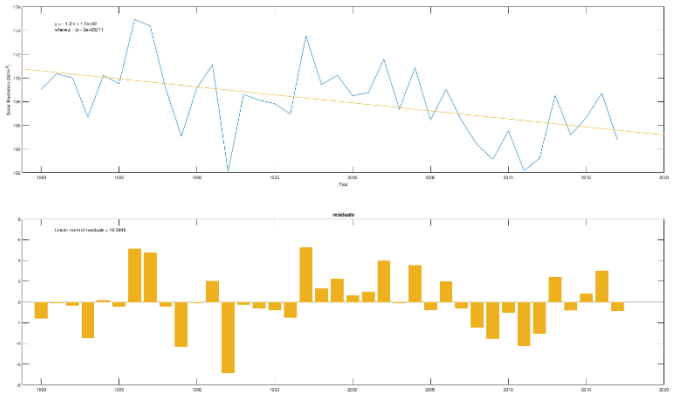

Figure A28 Ningxia Surface Incoming Solar Radiation 1980-2017

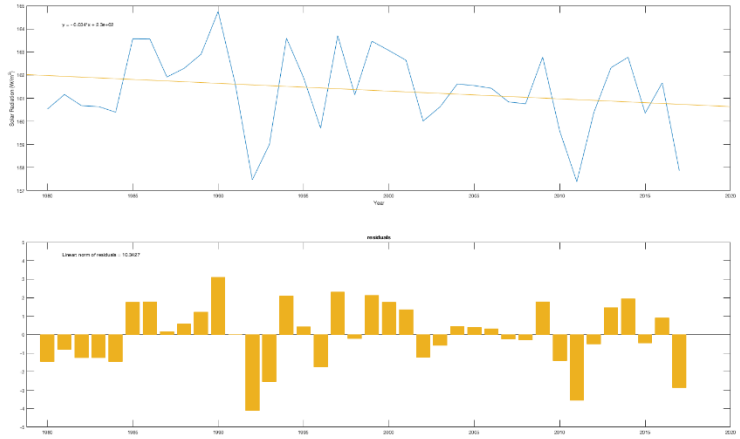

Figure A29 Xinjiang Surface Incoming Solar Radiation 1980-2017

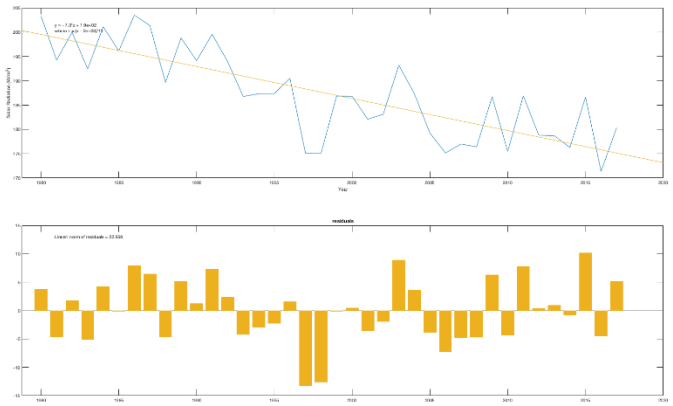

Figure A30 Hongkong Surface Incoming Solar Radiation 1980-2017

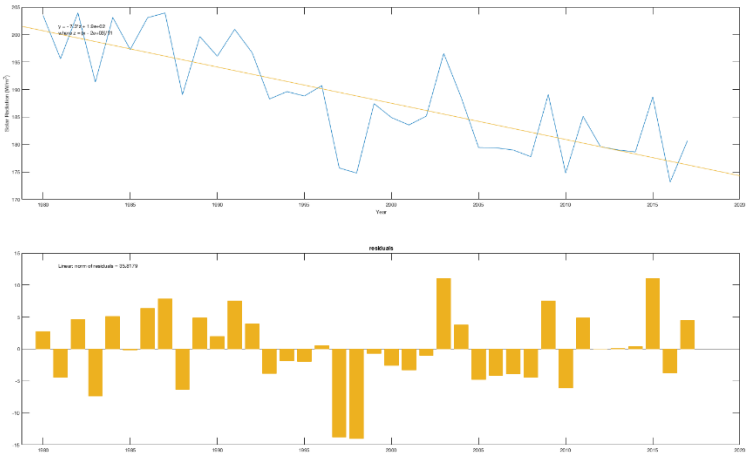

Figure A31 Macao Surface Incoming Solar Radiation 1980-2017

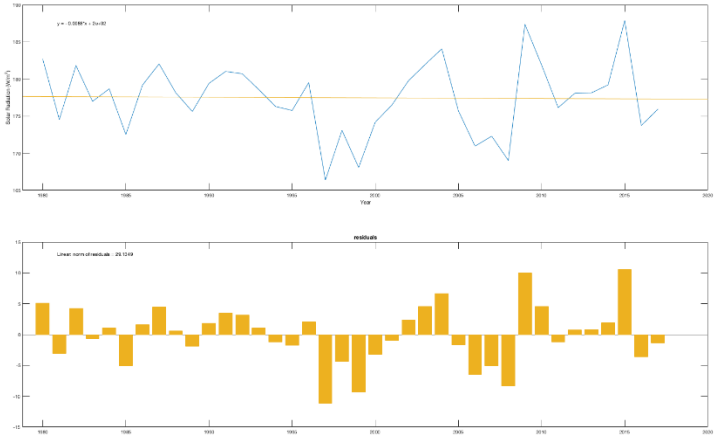

Figure A32 Taiwan Surface Incoming Solar Radiation 1980-2017